We are IntechOpen, the world's leading publisher of Open Access books Built by scientists, for scientists

4,800
Open access books available

122,000
International authors and editors

135M
Downloads

Our authors are among the

154
Countries delivered to

TOP 1%
most cited scientists

12.2%
Contributors from top 500 universities

CLARIVATE ANALYTICS BOOK CITATION INDEX INDEXED

WEB OF SCIENCE™

Selection of our books indexed in the Book Citation Index in Web of Science™ Core Collection (BKCI)

Interested in publishing with us?
Contact book.department@intechopen.com

Numbers displayed above are based on latest data collected.
For more information visit www.intechopen.com

8

Rolling Stability Control of In-wheel Motor Electric Vehicle Based on Disturbance Observer

Kiyotaka Kawashima, Toshiyuki Uchida and Yoichi Hori
University of Tokyo
Japan

1. Introduction

1.1 In-wheel-motor electric vehicle's advantages and application to vehicle motion control

Electric vehicles (EVs) with distributed in-wheel-motor systems attract global attention not only from the environmental point of view, but also from the vehicle motion control. In-wheel-motor EVs can realize high performance vehicle motion control by utilizing advantages of electric motors which internal combustion engines do not have. The EV has the following four remarkable advantages (Hori et al., 2004):

- Motor torque response is 10-100 times faster than internal combustion engine's one. This property enables high performance adhesion control, skid prevention and slip control.
- Motor torque can be measured easily by observing motor current. This property can be used for road condition estimation.
- Since an electric motor is compact and inexpensive, it can be equipped in each wheel. This feature realizes high performance three dimensional vehicle motion control.
- There is no difference between acceleration and deceleration control. This actuator advantage enables high performance braking control.

Slip prevention control is proposed utilizing fast torque response. Road condition and skid detection methods are developed utilizing the advantage that torque can be measured easily (Hori et al., 2004). Yawing stability control, side slip angle estimation and control methods are also proposed by utilizing a distributed in-wheel-motor system (Fujimoto et al., 2006 & 2007; Hori et al., 2007).

1.2 Background and purpose of the research

The purpose of this paper is to propose integrated rolling and yawing stability control (RSC and YSC). Rollover stability is important for all classes of light-vehicles such as light trucks, vans, SUVs and especially, for EVs which have narrow tread and high CG because EV is suitable for relatively small vehicle and human height does not change. According to the data from NHTSA, ratio of rollover accidents of pick ups' and vans' crashes in 2002 was only 3% against whole accidents. However, nearly 33% of all deaths from passenger vehicle crashes are due to rollover accidents (NHTSA, 2007).

Therefore, RSC is very important not only for ride quality but also for safety. The RSC system has been developed by several automotive makers and universities (Liebemann et

Source: Motion Control, Book edited by: Federico Casolo,
ISBN 978-953-7619-55-8, pp. 580, January 2010, INTECH, Croatia, downloaded from SCIYO.COM

al., 2004; Tseng et al., 2007; Yi et al., 2008). Rollover detection systems, such as rollover index (*RI*) (Yi et al., 2008) and Time-to- rollover (*TTR*) (Peng et al., 2001) are proposed for mitigating critical rolling motion. Every system controls braking force on each wheel independently and suppresses sudden increase of lateral acceleration or roll angle. However, since braking force is the average value by pulse width modulation control of brake pad, brake system cannot generate precise torque or positive torque. In the case of in-wheel-motor, both traction and braking force can be realized quickly and precisely. In addition to actuator advantages, RSC is designed by utilizing two-degrees-of-freedom (2-DOF) control based on disturbance observer (DOB) (Kawashima et al., 2008). For the vehicle motion control field, DOB is applied to vehicle yaw/pitch rate control (Fujimoto et al., 2006 & 2007) and 2-DOF control is applied to the electric power steering control (Guvenc et al., 2004). There are three reasons to utilize DOB: 1) disturbance suppression, 2) nominalize lateral vehicle model and 3) tracking capability to reference value. DOB loop that suppresses the effect of disturbance is faster than outer loop that achieves tracking capability. Designing DOB for traction force is not applicable for ICEV, because engine torque is not accurately known and long time delay exists. Therefore, DOB is applicable only in case of EVs. The tracking capability and robustness for lateral acceleration disturbance against such as side blast are realized by the proposed method. However, roll and yaw stabilities are incompatible. High rolling stability makes vehicle behavior under steer. On the other hand, high yawing stability to avoid vehicle side slip, vehicle roll stability is not guaranteed. In the next section, electronic stability program (ESP) on EV is introduced using *RI* based on vehicle geometry and dynamics model, which achieves integrated three dimensional vehicle motion control.

2. Electric stability program for electric vehicle

2.1 Introduction of electric stability program

Fig. 1. shows concept of ESP for EV. ESP consists of two systems; vehicle/road state estimation system (S1) and integrated vehicle motion control system (S2). S1 integrates

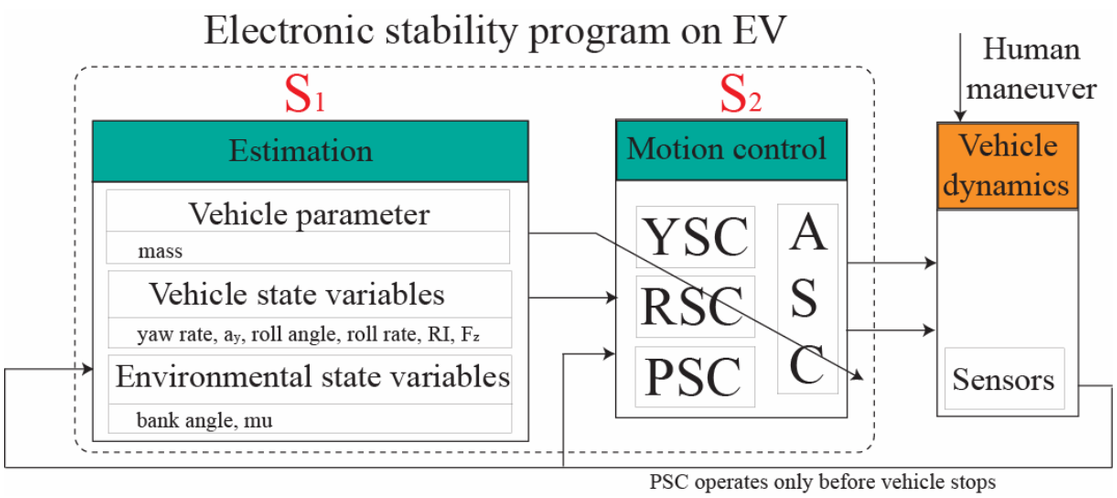

Fig. 1. EPS based on DOB

information from sensors (accelerometer, gyro, GPS, suspension stroke and steering angle sensors) and estimates unknown vehicle parameters (mass), vehicle state variables (yaw rate, lateral acceleration, roll angle, roll rate and normal forces on tires) and environmental state variables (Tseng et al., 2007; Hac et al., 2004). According to the information from S1, S2 controls vehicle dynamics using RSC and YSC, pitching stability control (PSC) and anti-slip control (ASC). According to *RI*, which is calculated by S1, a proper stability control strategy (YSC, RSC or mixed) is determined. RSC is based on DOB and nominal vehicle state is calculated by a controller. If there are errors between calculated and actual dynamics, it is compensated by differential torque.

2.2 A scheme of integrated vehicle motion control

Lateral acceleration is composed of vehicle side slip, yaw rate and longitudinal speed.

$$a_y = V(\dot{\beta} + \gamma) \tag{1}$$

If constant vehicle speed is assumed and lateral acceleration is suppressed, yaw rate is also suppressed as long as differentiation of side slip is not controlled. This physical constraint makes RSC and YSC incompatible. Therefore, rollover detection is necessary for integrated control. In order to detect rollover, Yi proposed *RI* ($0 < RI < 1$) as a rollover detection (Yi et al., 2008). When *RI* is high which means a vehicle is likely to roll over, the weight of RSC is set as high. On the other hand, *RI* is small, which means a vehicle is not likely to roll over, the weight of YSC is set as high. Control algorithm is simple and given by following equation. Fig. 2. shows block diagram of three dimensional integrated vehicle motion control.

$$\begin{aligned} N^* &= f(RI, N_{RSC}, N_{YSC}, N_{DOB}) \\ &= RI * N_{RSC} + (1 - RI) * N_{YSC} + N_{DOB} \end{aligned} \tag{2}$$

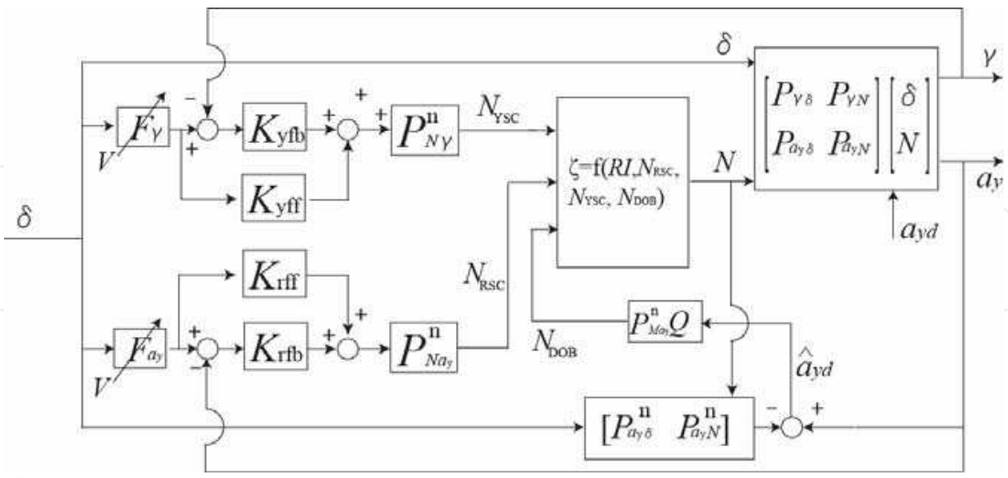

Fig. 2. Block diagram of integrated vehicle motion control

3. Estimation system

S1 is composed of vehicle parameters, state variables and environmental state variables estimation system. In this section, vehicle state variable estimation system is mainly

introduced. According to the estimated state variables, *RI*, a distribution ratio of RSC and YSC is determined.

3.1 Lateral acceleration and roll angle observer

Fig. 3. and fig. 4. show four wheel model and rolling model of electric vehicle.
Vehicle motion is expressed as the following three linear equations.

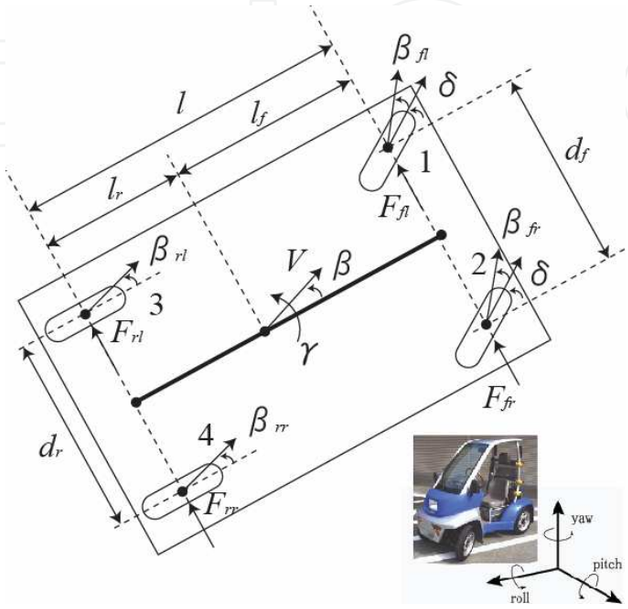

Fig. 3. Four wheel model

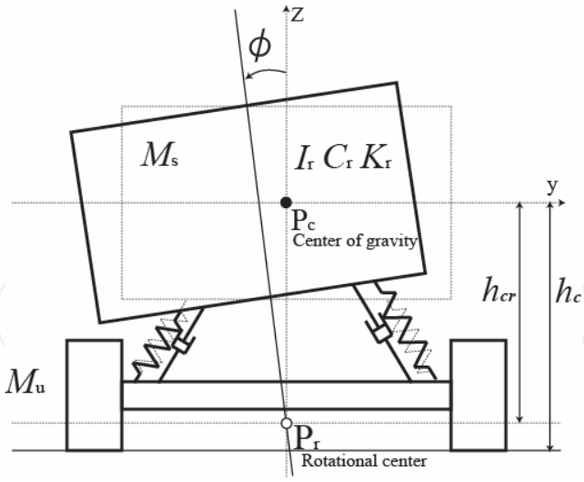

Fig. 4. Rolling model

Lateral motion:

$$\begin{aligned} MV(s\beta+\gamma) &= F_{yfl}+F_{yfr}+F_{yrl}+F_{yrr} \\ &= -2c_f(\beta+\frac{l_f}{V}\gamma-\delta)-2c_r(\beta-\frac{l_r}{V}\gamma) \end{aligned} \tag{3}$$

Yawing motion:

$$\begin{aligned} I_{yaw} s\gamma &= (F_{yfl} + F_{yfr}) l_f - (F_{yrl} + F_{yrr}) l_r \\ &= -2c_f (\beta + \frac{l_f}{V}\gamma - \delta) l_f + 2c_r (\beta - \frac{l_r}{V}\gamma) l_r + N \end{aligned} \tag{4}$$

Rolling motion:

$$M_s h_{cr} a_y = I_r \ddot{\phi} + C_r \dot{\phi} + K_r \phi - M_s g h_{cr} \sin\phi \quad (\phi < \phi_{wheel-lift-off}) \tag{5a}$$

$$M_s h_{cr} a_y = I_{r2} \ddot{\phi} - M_{sgh_{cr}} \sin\phi + M_s g \frac{d}{2} \cos\phi \quad (\phi > \phi_{wheel-lift-off}) \tag{5b}$$

Here, these motion equations need to be expressed as state equations to design observer. Observer gain matrix, however, becomes 2 * 4 matrix if whole equations are combined. To reduce redundancy of designing gain matrix, tire dynamics and rolling dynamics are separated. A matrix, A_{rt} connects two state equations. From eq.(3) and eq.(4), state equation is expressed as,

$$\dot{x}_t = A_t x_t + B_t u, \tag{6}$$

$$y_t = C_t x_t + D_t u. \tag{7}$$

It is noted that there is feedforward term in the transfer function from u to y_t. Therefore, to eliminate feedforward term and design stable observer, x_t vector is defined using differential torque and steering angle as the following equations,

$$\text{where}, x_t = \begin{bmatrix} a_y - c_2\delta & \dot{a}_y - c_2\dot{\delta} - b_1 N - c_1\delta \end{bmatrix}^T,$$

$$y_t = a_y, u = \begin{bmatrix} N & \delta \end{bmatrix},$$

$$A_t = \begin{bmatrix} 0 & 1 \\ -a_0 & -a_1 \end{bmatrix}, B_t = \begin{bmatrix} b_1 & c_1 \\ a_1 b_1 + b_0 & a_1 c_1 + c_0 \end{bmatrix},$$

$$C_t = \begin{bmatrix} 1 & 0 \end{bmatrix}, D_t = \begin{bmatrix} 0 & c_2 \end{bmatrix},$$

$$a_0 = \frac{4c_f c_r l^2}{MI_y V^2} - \frac{2(c_f l_f - c_r l_r)}{I_y}, a_1 = \frac{2M(c_f l_f^2 + c_r l_l^2) + 2I_y(c_f + c_r)}{MI_y V},$$

$$b_0 = \frac{2(c_f + c_r)}{MI_y}, b_1 = -\frac{2(c_f l_f - c_r l_r)}{MI_y V}, c_0^{'} = \frac{4c_f c_r l}{MI_y}, c_1^{'} = \frac{4c_f c_r l_r l}{MI_y V},$$

$$c_0 = c_0^{'} - a_0 c_2, c_1 = c_1^{'} - a_1 c_2, c_2 = \frac{2c_f}{N}.$$

From eq.(5a), state space equation is,

$$\dot{x}_r = A_r x_r + A_{rt} y_t, \tag{8}$$

$$y_r = C_r x_r, \tag{9}$$

$$\text{where, } x_t = \begin{bmatrix} \phi & \dot{\phi} \end{bmatrix}^T, \; y_r = \dot{\phi},$$

$$A_r = \begin{bmatrix} 0 & 1 \\ -\dfrac{K_r - M_s g h_{cr}}{I_r} & -\dfrac{C_r}{I_r} \end{bmatrix}, A_{rt} = \begin{bmatrix} 0 & 0 \\ \dfrac{M_s h_{cr}}{I_r} & 0 \end{bmatrix},$$

$$C_r = \begin{bmatrix} 0 & 1 \end{bmatrix}.$$

It should be noted that lateral acceleration dynamics expressed as eq.(6) is a linear time varying system depending on vehicle speed. The states are observable at various longitudinal speed except for a very low speed. In the following sections, for repeatability reason, experiment has been done under constant speed control. Observer gains are defined by pole assignment.

These parameters are based on the experiment vehicle"Capacitor-COMS1" developed in our research group. The method to evaluate the values of c_f, c_r are referred to the paper (Takahashi et al., 2006). Since rolling dynamics was unknown, model identification is conducted to derive roll model. Constant trace method is applied to the rolling model parameters identification. From equation (5a), lateral acceleration $\hat{a}_y$ is written as

$$\hat{a}_y(k \mid \theta) = \hat{\theta}^T \xi(k), \tag{10}$$

where, $\theta = [I_{roll} \quad C_{roll} \quad K_{roll}]^T$, $\xi = [\ddot{\phi} \quad \dot{\phi} \quad \phi]^T$.

The algorithm of the constant trace method is to update forgetting factor λ, such that trace of gain matrix P, is maintained as constant.

Due to the forgetting factor, when ξ is big, θ can be identified with good precision, and when ξ is small and little information, θ is seldom updated. With constant trace method, stable parameter estimation is achieved. Update equation is written by the following equation.

$$\varepsilon(k) = a_y(k) - \hat{\theta}^T(k-1)\xi(k) \tag{11}$$

$$\hat{\theta}(k) = \hat{\theta}(k-1) + \frac{P(k-1)\xi(k)}{1 + \xi^T(k)P(k-1)\xi(k)}\varepsilon(k) \tag{12}$$

$$P(k) = \frac{1}{\lambda(k)}\left\{P(k-1) - \frac{P(k-1)\xi(k)\xi^T(k)P(k-1)}{1 + \xi^T(k)P(k-1)\xi(k)}\right\} \tag{13}$$

$$\lambda(k) = 1 - \frac{|P(k-1)\xi(k)|}{1 + \xi^T(k)P(k)\xi(k)}\frac{1}{tr[P(0)]} \tag{14}$$

where, ε is output error.

Utilizing constant trace method to the experimental result, angular frequency $\sqrt{K_r / I_r}$ = 17.2 (rad/sec) and damping coefficient $\sqrt{1/(2I_r K_r)}C_r$ = 0.234 (1/sec). Fig. 5. shows detected acceleration information by sensor and calculated acceleration with estimated

parameter $\hat{\theta}$ and ξ. From the figure, the two lines merge and parameter identification is succeeded.

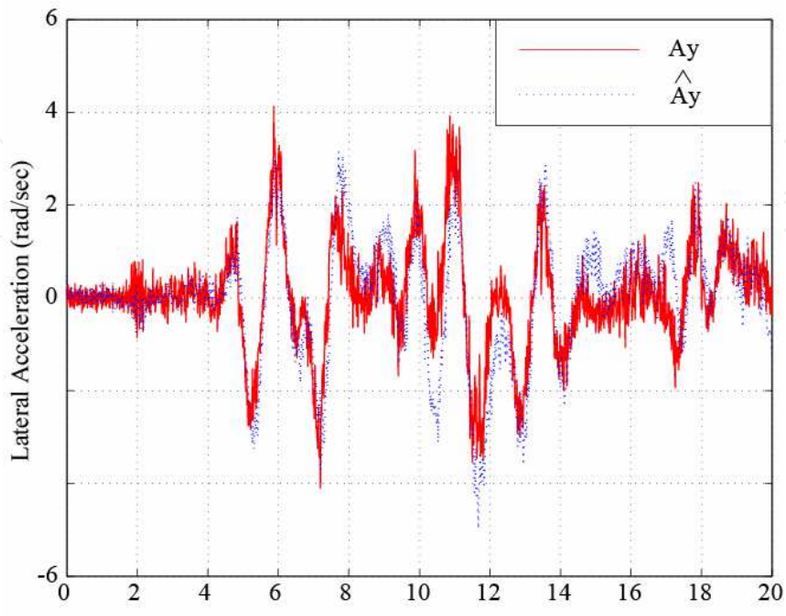

Fig. 5. Title of figure, left justified

3.2 Rollover index

RI is a dimensionless number which indicates a danger of vehicle rollover. *RI* is defined using the following three vehicle rolling state variables; 1)present state of roll angle and roll rate of the vehicle, 2)present lateral acceleration of the vehicle and 3)time-to-wheel lift. *RI* is expressed as eq. (15),

$$RI = C_1\left(\frac{|\phi|\dot{\phi}_{th} + \phi_{th}|\dot{\phi}|}{\phi_{th}\dot{\phi}_{th}}\right) + C_2\left(\frac{|a_y|}{a_y}\right) + (1 - C_1 - C_2)\left(\frac{|\phi|}{\sqrt{\phi^2 + \dot{\phi}^2}}\right), \quad if \quad \phi(\dot{\phi} - k_1\phi) > 0 \tag{15}$$

$$RI = 0, \quad else \quad if \quad \phi(\dot{\phi} - k_1\phi) < 0$$

where, *C*1,*C*2 and *k*1 are positive constants (0 < *C*1, *C*2 < 1). *ayth* is defined by vehicle geometry.

Fig. 6. shows equilibrium lateral acceleration in rollover of a suspended vehicle. It shows the relation between vehicle geometry such as h, d and K_r and vehicle states such as ϕ and a_y. From the static rollover analysis, critical lateral acceleration a_{yth} which induces rollover is defined. Phase plane analysis is conducted using a_{yth} and roll dynamics.

Fig. 7. shows phase plane plot under several initial condition $(\phi, \dot{\phi})$ at critical lateral acceleration. Consequently, ϕ_{th} and $\dot{\phi}_{th}$ are defined by the analysis.

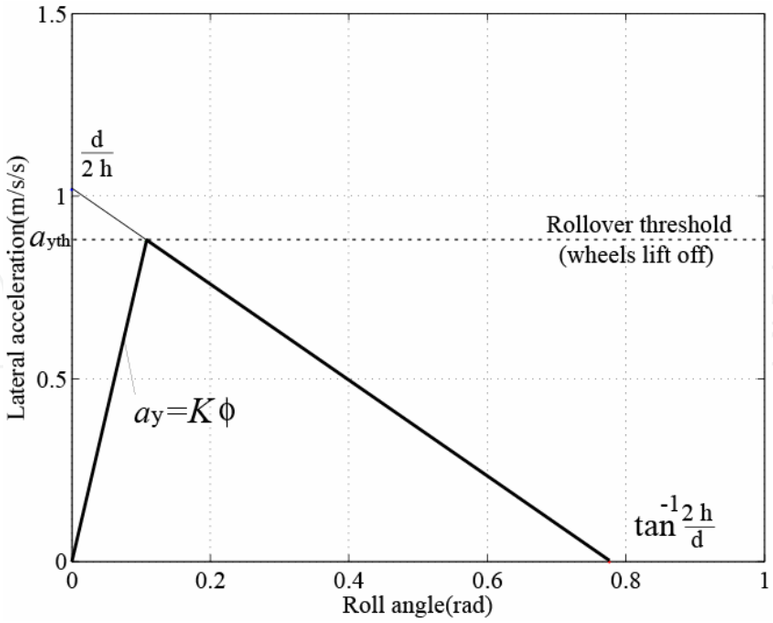

Fig. 6. Equilibrium lateral acceleration in rollover of a suspended vehicle

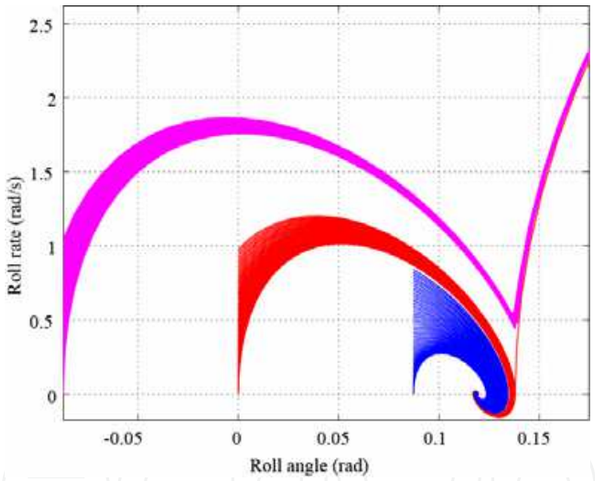

Fig. 7. Phase plane plot of roll dynamics

4. Integrated motion control system

4.1 Rolling stability control based on two-degree-of-freedom control

In this section, RSC based on 2-DOF control which achieves tracking capability to reference value and disturbance suppression is introduced. For RSC, lateral acceleration is selected as controlling parameter because roll angle information is relatively slow due to roll dynamics (about 100ms).

(a) Lateral acceleration disturbance observer

Based on fig. 8., transfer function from reference lateral acceleration u, δ and a_{yth} to a_y is expressed as the following equation. Roll moment is applied by differential torque N^* by

right and left in-wheel-motors. Reference value of lateral acceleration is given by steering angle and vehicle speed.

$$a_y = \frac{P_{a_yN} P^n_{Na_y} (K_{ff} + K_{fb})}{1 + P_{a_yN} P^n_{Na_y} K_{fb}} u + \frac{P_{a_y\delta}}{1 + P_{a_yN} P^n_{Na_y} K_{fb}} \delta + \frac{1}{1 + P_{a_yN} P^n_{Na_y} K_{fb}} a_{yd}. \tag{16}$$

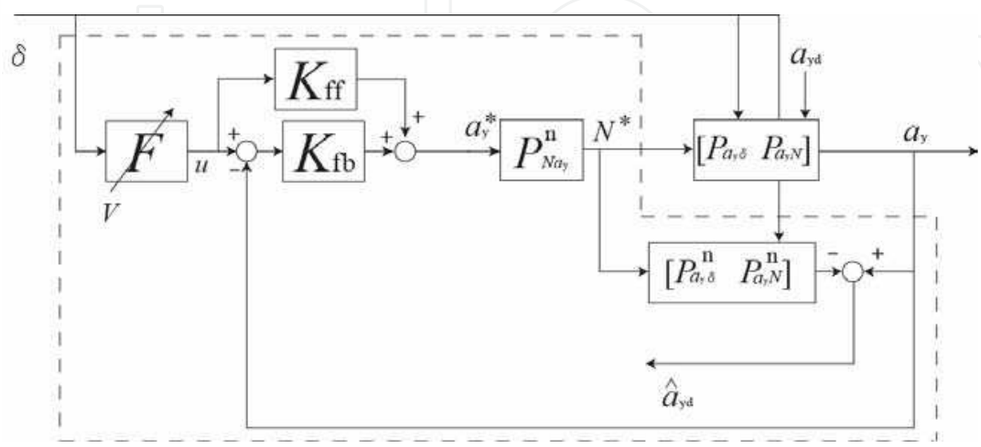

Fig. 8. Block diagram of lateral acceleration DOB

Tracking capability and disturbance suppression are two important performances in dynamics system control and can be controlled independently. On the other hand, one-degree-of-freedom (1-DOF) control such as PID controller loses important information at subtracting actual value from reference one. In the control, there is only one way to se feedback gain as high to improve disturbance suppression performance, however the gain makes the system unstable. Hence 2-DOF control in terms of tracking capability and disturbance suppression is applied to RSC. Proposed lateral acceleration DOB estimates external disturbance to the system using information; V, δ, N and a_y.

Fig. 8. also shows the block diagram of lateral acceleration DOB.
Estimated lateral acceleration disturbance $\hat{a}_{yth}$ and a_y are expressed as

$$\hat{a}_{yd} = a_y - P^n_{a_yN} N^* - P^n_{a_y\delta} \delta, \tag{17}$$

$$a_y = P_{a_yN} N^* + P_{a_y\delta} \delta + a_{yd}. \tag{18}$$

$$\hat{a}_{yd} = \frac{P^n_{Na_y}}{P_{Na_y}} \left(\left(\frac{P_{Na_y}}{P^n_{Na_y}} - 1 \right) a_y + (P_{a_y\delta} - P^n_{a_y\delta}) \delta + a_{yd} \right). \tag{19}$$

In eq. (19), the first and the second terms are modeling errors and the third term is lateral disturbance. If modeling error is small enough, $\hat{a}_{yth}$ is approximately equal to actual lateral acceleration disturbance.

(b) Disturbance suppression and normalize of roll model

Fig. 9. shows the proposed 2-DOF control for RSC.

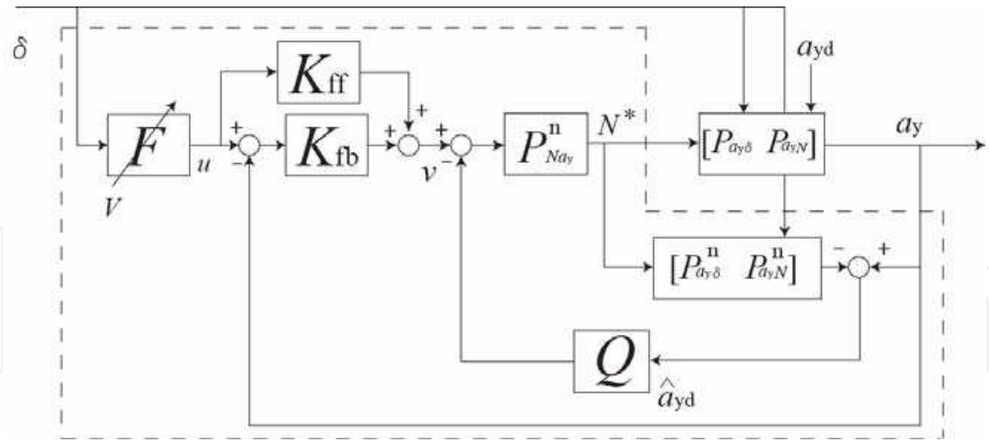

Fig. 9. Block diagram of 2-DOF for RSC based on DOB

Estimated lateral acceleration disturbance is fedback to lateral acceleration reference multiplied by filter Q.

$$a_y^* = v - Q\hat{a}_{yd.} \tag{20}$$

Filter Q is low pass filter and expressed as the following equation (Umeno et al., 1991). In this study, the cut-off frequency is set as 63 rad/s.

$$Q = \frac{1 + \sum_{k=1}^{N-r} a_k (\tau s)^k}{1 + \sum_{k=1}^{N} a_k (\tau s)^k}, \tag{21}$$

where, r must be equal or greater than relative order of the transfer function of the nominal plant. Substituting eq. (19) to eq. (17) and (20), the following equation is defined.

$$a_y = v + P^n_{a_y\delta}\delta + (1-Q)\hat{a}_{yd}. \tag{22}$$

Disturbance, which is lower than the cut-off frequency of Q and vehicle dynamics, is suppressed by DOB. In addition to the function of disturbance rejection, the plant is nearly equal to nominal model in lower frequency region than the cut-off frequency. Therefore the proposed RSC has the function of model following control.

4.2 Yawing stability control

As fig. 2. shows, YSC is yaw rate control. Yaw rate reference value is defined by steering angle and longitudinal vehicle speed. Transfer function from yaw rate reference and steering angle is expressed as the following equation.

$$\gamma = \frac{P_{\gamma M} P^n_{N\gamma}(K_{ff} + K_{fb})}{1 + P_{\gamma N} P^n_{N\gamma} K_{fb}} u + \frac{P_{\gamma\delta}}{1 + P_{\gamma N} P^n_{N\gamma} K_{fb}} \delta. \tag{23}$$

5. Simulation results

Three dimensional vehicle motion simulations have been conducted with combination software of CarSim 7.1.1 and MATLAB R2006b/Simulink. At first, the effectiveness of RSC is verified. Lateral acceleration disturbance is generated by differential torque for repeatability reason of experiments. In the simulation, lateral blast is generated at straight and curve road driving, the proposed DOB suppresses the disturbance effectively. To show the effectiveness of ESP, lateral acceleration response and trajectory at curving are compared. It is shown that lateral acceleration is unnecessarily suppressed only with RSC, however, tracking capability to yaw rate reference is achieved by ESP.

5.1 Effectiveness of RSC

(a)Vehicle Stability under Crosswind Disturbance

Vehicle stability of RSC under crosswind disturbance is demonstrated. At first, the vehicle goes straight and a driver holds steering angle (holding steering wheel as 0 deg). Under 20 km/h vehicle speed control, crosswind is applied during 3-6 sec. Fig. 10. shows the simulation results.

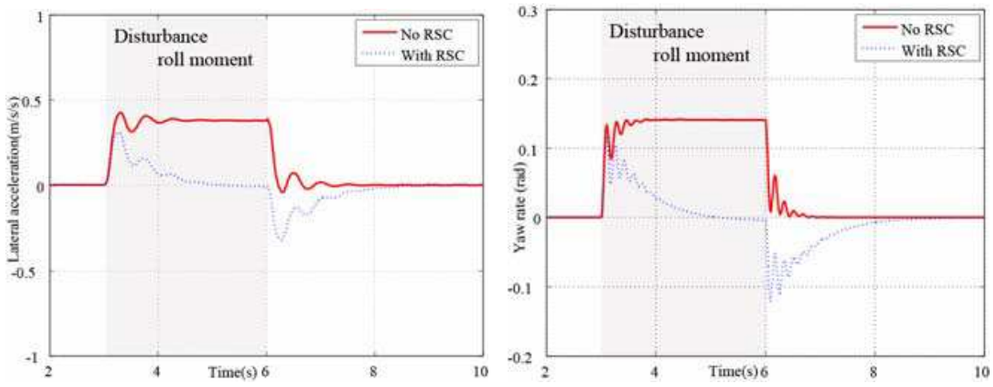

(a) Lateral acceleration (b) Yaw rate

Fig. 10. Simulation result of RSC: Disturbance suppression at straight road driving

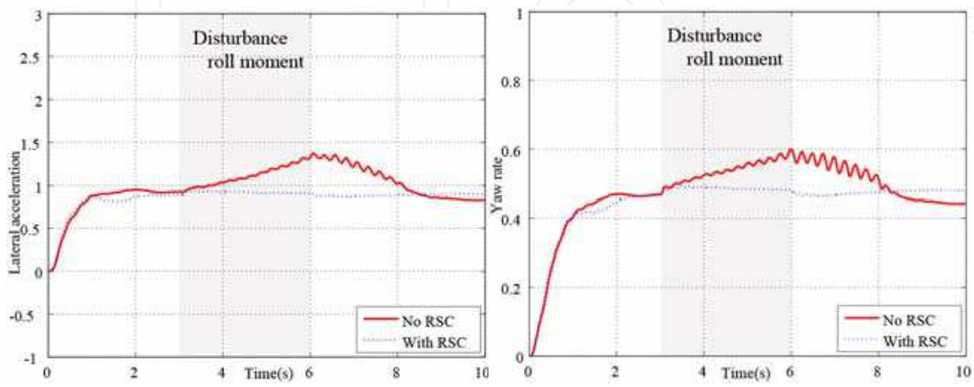

(a) Lateral acceleration (b) Yaw rate

Fig. 11. Simulation result of RSC: Disturbance suppression at curve road driving

When proposed RSC is activated, the proposed lateral acceleration DOB detects the lateral acceleration disturbance and suppresses it. Then, disturbance is applied at curve road driving. Under 20km/h constant speed control as well, 180 deg step steering is applied with roll moment disturbance during 3-6 sec. Fig. 11. shows decrease of lateral acceleration since disturbance is rejected perfectly by differential torque with RSC. The robustness of RSC is verified with simulation results.

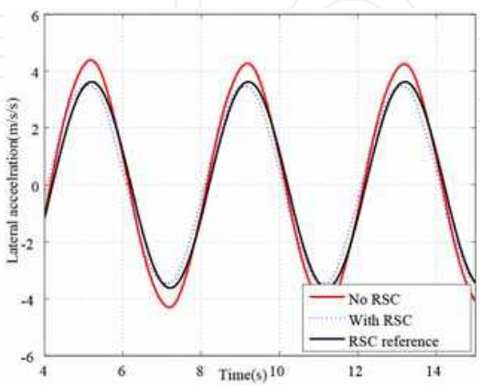

Fig. 12. Simulation result of RSC: Tracking capability to reference value

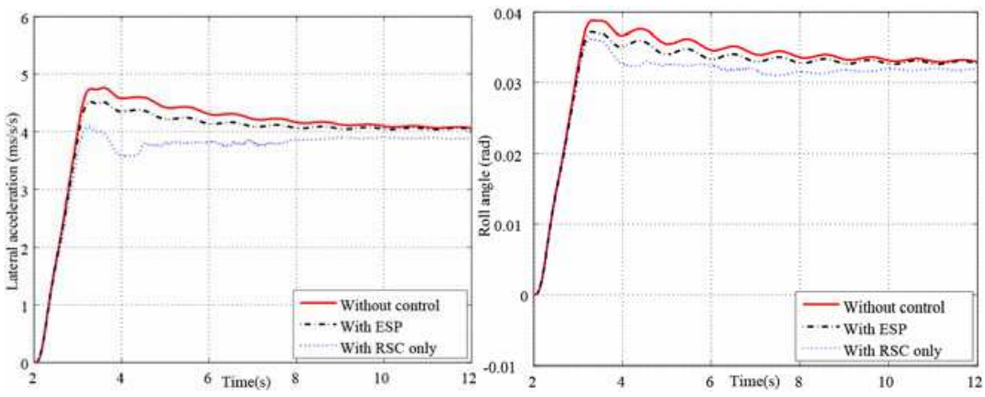

(a) Lateral acceleration (b) Roll angle

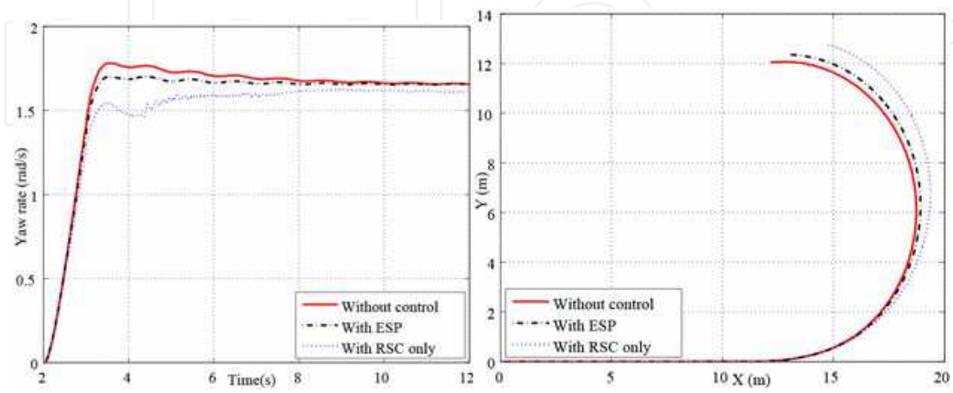

(c) Yaw rate (d) Trajectory

Fig. 13. Simulation results of ESP: Step steering maneuver

(b)Tracking capability to reference value

In this section, tracking capability of RSC to reference value is verified with simulation results. Under 20km/h vehicle speed control, 180 deg sinusoidal steering is applied and reference value of lateral acceleration is 80% of nominal value. Fig. 12. shows that lateral acceleration follows reference value with RSC.

5.2 Effectiveness of EPS

Rollover experiment can not be achieved because of safety reason. Under 20km/h constant speed control, 240 deg step steering is applied. From fig. 13., with only RSC case, even though the danger of rollover is not so high, lateral acceleration is strongly suppressed and trajectory of the vehicle is far off the road. On the other hand, with ESP case, the rise of lateral acceleration is recovered and steady state yaw rate is controlled so that it becomes close to no control case.

6. Experimental results

6.1 Experimental setup

A novel one seater micro EV named "Capacitor COMS1" is developed for vehicle motion control experiments. The vehicle equips two in-wheel motors in the rear tires, a steering sensor, an acceleration sensor and gyro sensors to detect roll and yaw motion. An upper micro controller collects sensor information with A/D converters, calculates reference torques and outputs to the inverter with DA converter. In this system, sampling time is 1 (msec). Fig. 14. shows the vehicle control system and Table 1. shows the specifications of the experimental vehicle.

At first, disturbance suppression performance and tracking capability to reference value are verified with experimental results. Then, effectiveness of ESP is demonstrated. In the experiment, since vehicle rollover experiment is not possible due to safety reason, step response of lateral acceleration and yaw rate are evaluated.

6.2 Effectiveness of RSC

(a)Vehicle Stability under Crosswind Disturbance

For repeatability reason, roll moment disturbance is generated by differential torque. Under 20 km/h constant speed control, roll moment disturbance is applied from 1 sec. The disturbance is detected by DOB and compensated by differential torque of right and left inwheel motors. Here, the cut-off frequency of the low pass filter is 63 rad/s.

Fig. 15. shows disturbance suppression during straight road driving. Step disturbance roll moment (equivalent to $0.5\,m/s^2 * h_{cr}$) is applied around 1 sec. In the case without any control and only with FB control of RSC, lateral acceleration is not eliminated and vehicle trajectory is shifted in a wide range. On the other hand, in the case with DOB, disturbance is suppressed and vehicle trajectory is maintained.

Fig. 16. shows the experimental results of disturbance suppression at curve road driving. Under 20 km/h constant speed control, 240 deg steering is applied and disturbance is applied at around 2.5 sec. In this case, data is normalized by maximum lateral acceleration. In the case with RSC DOB, whole effect of disturbance is suppressed as no disturbance case. In the case without RSC, lateral acceleration decreases about 25% and vehicle behavior becomes unstable.

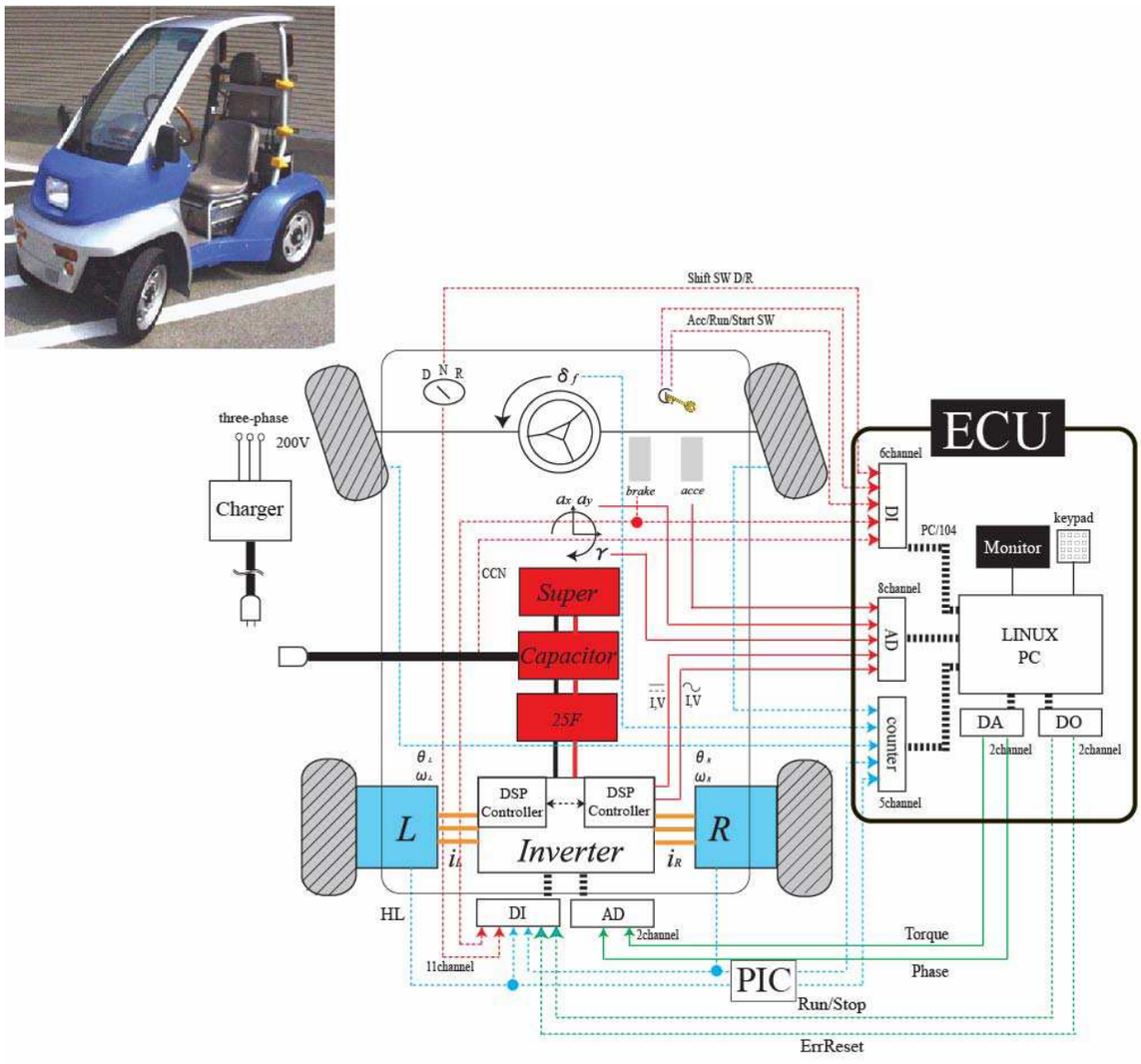

Fig. 14. Control system of experimental vehicle

Motor	
Category	IPMSM
Phase/Pole	3/12
Rating power/Max	0.29kW/2kW
Max torque	100Nm
Max velocity	50km/h
Inverter	
Switching Hardware	MOS FET
Control method	PWM vector control

Table 1. Drive train specification of experimental vehicle

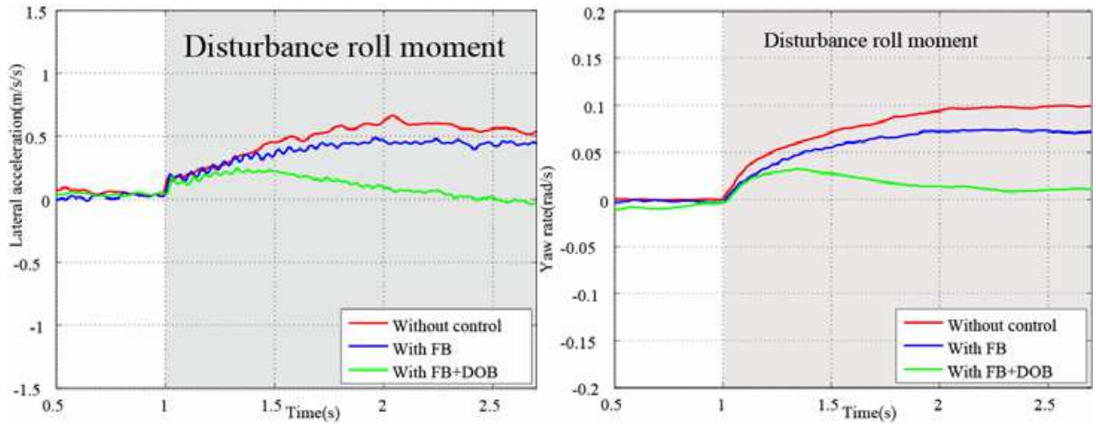

(a) Lateral acceleration (b) Yaw rate

Fig. 15. Experimental result of RSC: Disturbance suppression at straight road driving

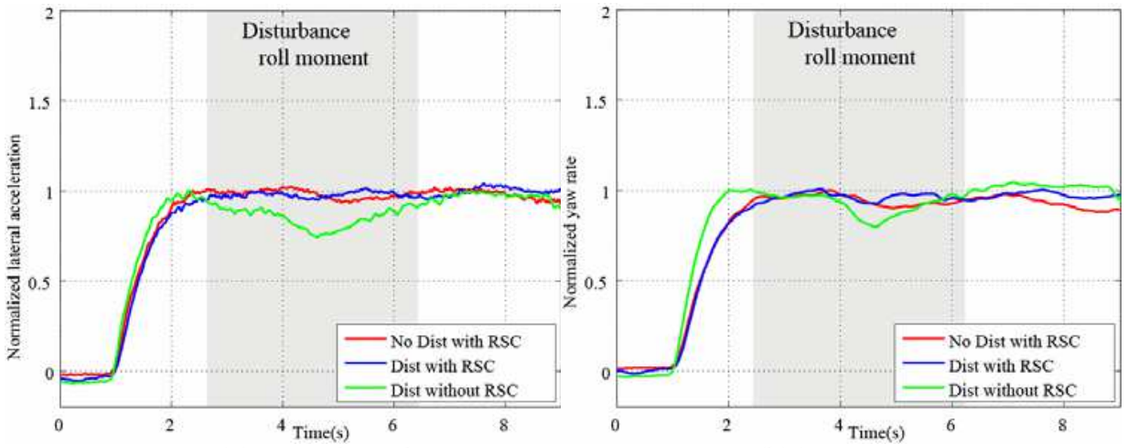

(a) Lateral acceleration (b) Yaw rate

Fig. 16. Experimental result of RSC: Disturbance suppression at curve road driving

(b)Tracking capability to reference value

In the previous section, since it was assured that the inner DOB loop is designed properly, tracking capability to reference value is verified with experimental results. 180 deg sinusoidal steering is applied and reference lateral acceleration is 80% of nominal value. The outer loop is designed with pole root loci method. Fig. 17. shows that in the case with RSC, tracking capability to reference value is achieved.

6.3 Effectiveness of EPS

Effectiveness of ESP is demonstrated by experiments. For safety reason, rollover experiment is impossible. Therefore, experimental condition is the same as 5.2. Under 20km/h constant speed control, 180 deg step steering is applied.

Fig. 18. shows that in the case with only RSC, lateral acceleration and yaw rate are strongly suppressed. On the other hand, in the case with ESP, yaw rate is recovered close to reference value. In addition, the rise of lateral acceleration is also recovered and stable cornering is achieved with ESP.

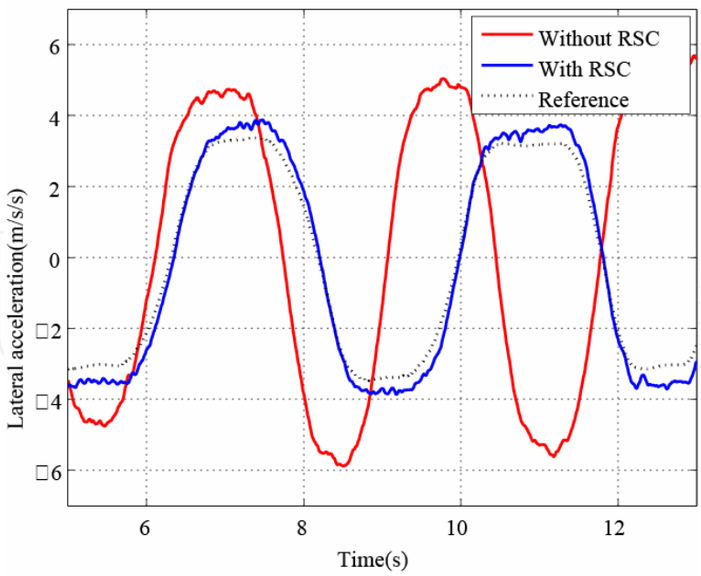

Fig. 17. Experimental result of RSC: Tracking capability to reference value

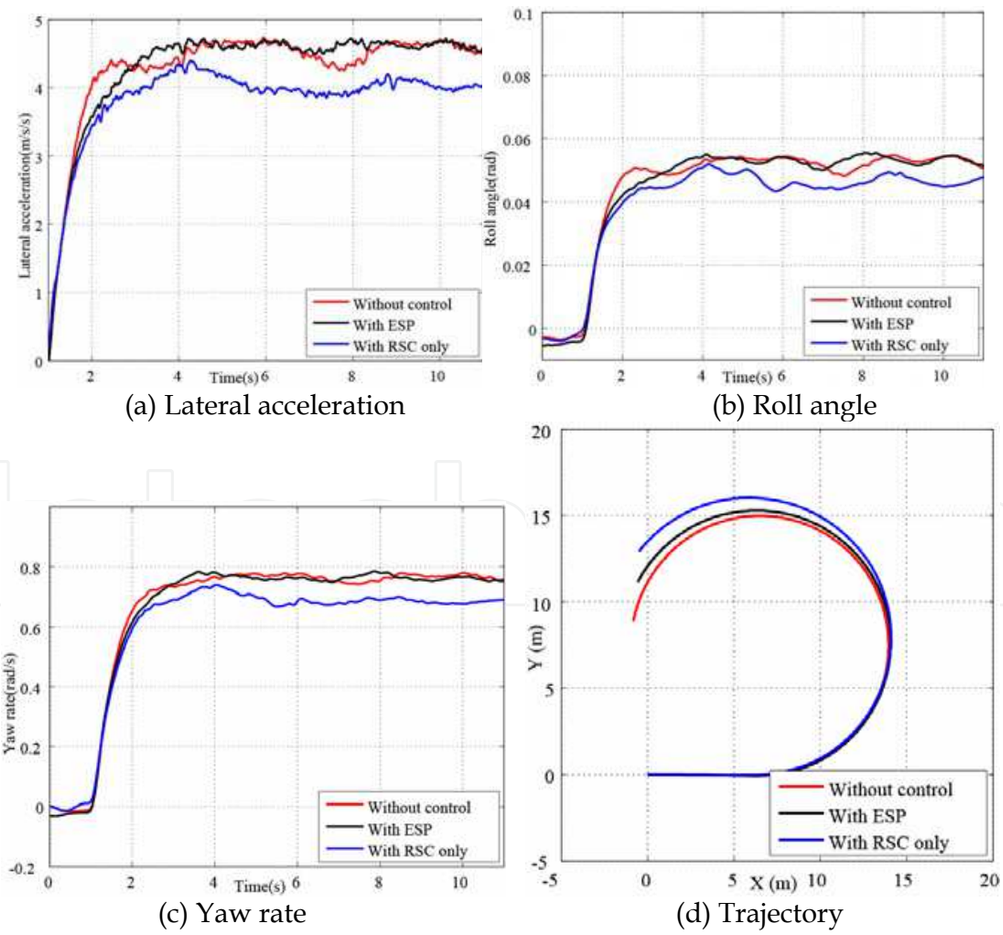

(a) Lateral acceleration (b) Roll angle

(c) Yaw rate (d) Trajectory

Fig. 18. Simulation results of ESP: Step steering maneuver

7. Conclusion

In this paper, a novel RSC based on ESP utilizing differential torque of in-wheel-motor EV is proposed. Effectiveness of novel RSC designed by 2-DOF control is verified with simulation and experimental results. Then incompatibility of RSC and YSC is described and ESP is proposed to solve the problem utilizing *RI* which is calculated using estimated value of estimation system of ESP. Experimental results validates the proposed ESP.

8. Acknowledgement

The author and the work are supported by Japan Society for the Promotion of Science.

9. References

Yoichi Hori, "Future Vehicle driven by Electricity and Control-Research on Four Wheel Motored UOT Electric March II", IEEE Transaction on Industrial Electronics, Vol.51, No.5, pp.954-962, 2004.10

Hiroshi Fujimoto, Akio Tsumasaka, Toshihiko Noguchi, "Vehicle Stability Control of Small Electric Vehicle on Snowy Road", JSAE Review of Automotive Engineers, Vol. 27, No. 2, pp. 279-286, 2006.04

Shinsuke Satou, Hiroshi Fujimoto, "Proposal of Pitching Control for Electric Vehicle with In-Wheel Motor", IIC-07- 81 IEE Japan, pp.65-70, 2007.03 (in Japanese).

Peng He, Yoichi Hori, "Improvement of EV Maneuverability and Safety by Dynamic Force Distribution with Disturbance Observer", WEVA-Journal, Vol.1, pp.258-263, 2007.05

National highway traffic safety administration, Safercar program, http://www.nhtsa.gov/

E. K. Liebemann, "Safety and Performance Enhancement: The Bosch Electronic Stability Control(ESP)", SAE Technical Paper Series, 2004-21-0060, 2004.10

Hongtei E. Tseng, et al, "Estimation of land vehicle roll and pitch angles", Vehicle System Dynamics, Vol.45, No.5, pp.433-443, 2007.05

Kyongsu Yi, et al, "Unified Chassis Control for Rollover Prevention, Maneuverability and Lateral Stability", AVEC2008, pp.708-713, 2008.10

Bo-Chiuan Chen, Huei Peng, "Differential-Braking-Based Rollover Prevention for Sport Utility Vehicles with Human-in- the-loop Evaluations", Vehicle System Dynamics, Vol.36, No.4-5, pp359-389, 2001.

Kiyotaka Kawashima, Toshiyuki Uchida, Yoichi Hori, "Rolling Stability Control of In-wheel Electric Vehicle Based on Two-Degree-of-Freedom Control", The 10th International Workshop on Advanced Motion Control, pp. 751-756, Trento Italy, 2008.03

Bilin Aksun Guvenc, Tilman Bunte, Dirk Odenthal and Levent Guvenc, "Robust Two Degree-of-Freedom Vehicle Steering Controller Design", IEEE Transaction on Control Systems Technology, Vol. 12, No. 4, pp.627-636, 2004.07

A. Hac, et. al, "Detection of Vehicle Rollover", SAE Technical Paper Series, 2004-01-1757, SAEWorld Congress, 2004.

N. Takahashi, et. al, "Consideration on Yaw Rate Control for Electric Vehicle Based on Cornering Stiffness and Body Slip Angle Estimation", IEE Japan, IIC-06-04, pp.17-22, 2006

Takaji Umeno, Yoichi Hori, "Robust Speed Control of DC Servomotors Using Modern Two Degrees-of-Freedom Controller Design", IEEE Transaction Industrial Electronics, Vol.38, No. 5, pp.363-368, 1991.10

Nomenclature

a_x, a_y : Longitudinal and lateral acceleration

a_{yd} : Lateral acceleration disturbance

a_{yth} : Critical lateral acceleration

c_f, c_r : Front and rear tire cornering stiffness

C_r : Combined roll damping coefficient

d, d_f, d_r : Tread at CG, front and rear axle

$F_{yfl}, F_{yfr}, F_{yrl}, F_{yrr}$: Tire lateral forces

g : Gravity acceleration

h_c, h_{cr} : Hight of CG and distance from CG to roll center

I_r, I_{r2} : Moment of inertia about roll axis (before and after wheel-lift-off)

I_y : Moment of inertia about yaw axis

K_r : Combined roll stiffness coefficient

l, l_f, l_r : Wheelbase and distance from CG to front and rear axle

M, M_s, M_u : Vehicle, sprung and unsprung mass

N : Yaw moment by differential torque

V, V_w : Vehicle and wheel speed

β, γ, δ : Body slip angle, yaw rate and tire steering angle

$\phi, \dot{\phi}, \phi_{th}, \dot{\phi}_{th}$: Roll angle, roll rate, threshold of roll angle and roll rate

Motion Control

Edited by Federico Casolo

ISBN 978-953-7619-55-8
Hard cover, 590 pages
Publisher InTech
Published online 01, January, 2010
Published in print edition January, 2010

The book reveals many different aspects of motion control and a wide multiplicity of approaches to the problem as well. Despite the number of examples, however, this volume is not meant to be exhaustive: it intends to offer some original insights for all researchers who will hopefully make their experience available for a forthcoming publication on the subject.

How to reference

In order to correctly reference this scholarly work, feel free to copy and paste the following:

Kiyotaka Kawashima, Toshiyuki Uchida and Yoichi Hori (2010). Rolling Stability Control of In-wheel Motor Electric Vehicle Based on Disturbance Observer, Motion Control, Federico Casolo (Ed.), ISBN: 978-953-7619-55-8, InTech, Available from: http://www.intechopen.com/books/motion-control/rolling-stability-control-of-in-wheel-motor-electric-vehicle-based-on-disturbance-observer

INTECH
open science | open minds

InTech Europe
University Campus STeP Ri
Slavka Krautzeka 83/A
51000 Rijeka, Croatia
Phone: +385 (51) 770 447
Fax: +385 (51) 686 166
www.intechopen.com

InTech China
Unit 405, Office Block, Hotel Equatorial Shanghai
No.65, Yan An Road (West), Shanghai, 200040, China
中国上海市延安西路65号上海国际贵都大饭店办公楼405单元
Phone: +86-21-62489820
Fax: +86-21-62489821

IntechOpen